J. Membrane Biol. 146, 263–272 (1995)

The Journal of
Membrane
Biology



# Patch Clamp and Atomic Force Microscopy Demonstrate TATA-Binding Protein (TBP) Interactions with the Nuclear Pore Complex

**J.O. Bustamante[1,2], A. Liepins[3], R.A. Prendergast[3], J.A. Hanover[4], H. Oberleithner[5]**

[1]University of Maryland School of Medicine, Department of Physiology, Baltimore, MD 21201
[2]Memorial University of Newfoundland, School of Medicine, Division of Basic Medical Sciences, St. John's, Newfoundland, Canada A1B 3V6
[3]Johns Hopkins University, Wilmer Eye Institute, Baltimore, MD 21287
[4]Laboratory of Biochemistry and Metabolism, National Institute of Diabetes and Digestive and Kidney Diseases, National Institutes of Health, Bethesda, MD 20892
[5]Physiologisches Institut der Universität Würzburg, D 97070, Würzburg, Germany

Received: 30 August 1994/Revised: 19 April 1995

**Abstract.** The universal TATA-binding protein, TBP, is an essential component of the multiprotein complex known as transcription factor IID (TFIID). This complex, which consists of TBP and TBP-associated factors (TAFs), is essential for RNA polymerase II-mediated transcription. The molecular size of human TBP (37.7 kD) is close to the passive diffusion limit along the transport channel of the nuclear pore complex (NPC). Therefore, the possibility exists that NPCs restrict TBP translocation to the nuclear interior. Here we show for the first time, with patch-clamp and atomic force microscopy (AFM), that NPCs regulate TBP movement into the nucleus and that TBP ($10^{-15}$–$10^{-10}$ M) is capable of modifying NPC structure and function. The translocation of TBP was ATP-dependent and could be detected as a transient plugging of the NPC channels, with a concomitant transient reduction in single NPC channel conductance, $\gamma$, to a negligible value. NPC unplugging was accompanied by permanent channel opening at concentrations greater than 250 pM. AFM images demonstrated that the TBP molecules attached to and accumulated on the NPC cytosolic side. NPC channel activity could be recorded for more than 48 hr. These observations suggest that three novel functions of TBP are: to stabilize NPC, to force the NPC channels into an open state, and to increase the number of functional channels. Since TBP is a major component of transcription, our observations are relevant to the understanding of the gene expression mechanisms underlying normal and pathological cell structure and function.

*Correspondence to:* J.O. Bustamante

**Key words:** Nuclear pore complex — Nuclear ion channels — Gene activity — Control of gene expression — TATA-binding protein — TBP — Patch clamp — Atomic force microscopy — Cell nucleus

## Introduction

TFIID, which consists of the universal TATA-binding protein (TBP, i.e, Hernandez, 1993; Kim & Burley, 1994; Nikolov & Burley, 1994; Struhl, 1994) and TBP-associated factors (TAFs, e.g., Tanese & Tjian, 1993), plays a major role in basal and stimulated gene expression (Horikoshi et al., 1989; Lewin, 1990; Greenblatt, 1992; Conaway & Conaway, 1993; Buratowski, 1994; Hori & Carey, 1994; Kokubo et al., 1994; Rowlands et al., 1994). Increased recruitment of TBP to the promoter by transcriptional activation domains has been reported *in vivo* (Klein & Struhl, 1994). TBP, like other transcription factors, is known to multimerize (e.g., Kato et al. 1994; Tjian & Maniatis, 1994). As a nuclear protein, TBP uses the NPC channel to gain access to its binding site in the DNA molecule. Since the size of human TBP is close to the cutoff limit for passive diffusion through NPCs (≈40 kD; e.g., Miller et al., 1991), TBP alone or multimerized has the potential of plugging the nuclear pore during translocation and, thus, of reducing NPC ion conductance, $\gamma$. In the previous companion paper (Bustamante et al., 1995*a*) we showed that $\gamma$ is blocked by two agents known to prevent macromolecular translocation along the NPC channel: wheat germ agglutinin and mAb414, a monoclonal antibody to a nuclear pore pro-

tein. We also showed that the behavior of NPCs as ion channels is minimized during translocation of large macromolecules along the channel because the macromolecules interrupt ion flow along the channel (Bustamante et al., 1995*b*). Therefore, macromolecular translocation along the NPC channel can be detected with patch clamp (Bustamante et al., 1995*a,b*).

NPCs and transcription factors (TFs) contain *O*-linked *N*-acetylglucosamine (*O*-GlcNAc) moieties (e.g., Holt et al., 1987; Jackson & Tjian, 1988). Since glycoproteins modified this way are known to form multimers (Hart et al., 1989; Haltiwanger et al., 1992*a,b*), we hypothesized that TBP could bind to NPCs. The large size of TBP and its multimers should be a good target for high-resolution imaging techniques such as atomic force microscopy (AFM, Binning et al., 1986; Rutgar & Hansma, 1990). AFM is one of several scanning probe microscopy techniques introduced during the past decade (e.g., Engel, 1991; Hoh & Hansma, 1992; Radmacher et al., 1992; Morris, 1994). This technique has been successfully used to observe the topology of several ion channels (*reviewed in* Lal et al., 1993; Lal & John, 1994), including gap junctional channels (e.g., Hoh et al., 1991, 1993), acetylcholine receptors (e.g., Lal & Yu, 1993) and, recently, NPCs (e.g., Braunstein & Spudich, 1994; Oberleithner et al., 1994; Panté & Aebi, 1994). In the present work we have combined out patch clamp and AFM resources to test the hypotheses that NPCs regulate TBP translocation to the nuclear interior and that TBP affects NPCs through direct interactions. Our experimental results demonstrate that TBP movement into the nuclear compartment is regulated by NPCs and that TBP molecules bind and modify NPCs, conferring them increased mean conductance and stability. These novel observations are relevant to the understanding of nuclear processes (e.g., transcriptional control and gene expression) and, therefore, they are helpful in identifying the mechanisms underlying normal and pathological cell structure and function.

## Materials and Methods

### Nuclei, Solutions, Patch Clamp

Details of the procedures for nuclei isolation and patch-clamping were given in the two preceding companion papers (Bustamante et al., 1995*a,b*).

### TATA-binding Protein, TBP

TBP was expressed in *Escherichia coli* from full-length human cDNA clones (Promega). Test solutions were prepared as described in the preceding paper (Bustamante et al., 1995*b*). Briefly, the TBP-containing solution was prepared in high-K saline (mM: 150 KCl, 5 $MgCl_2$, 10 HEPES, 4 KOH, pH 7.2–7.3, 21–24°C). A consensus oligonucleotide recognizing the TATA-binding protein was used: 5′-GCAGAGCATATAAGGTGAGGTAGG-A-3′ and 3′-CGTCTCG-TATATTCCACTC-CATCCT-5′, Promega).[1]

### Atomic Force Microscopy

AFM procedures have been recently described (Oberleithner et al., 1993, 1994). Briefly, kidney cell nuclei were incubated in the high-K solution containing 1 pM TBP and 2 mM ATP. AFM images were taken in the saline-containing perfusion chamber ("fluid-cell") of a Nanoscope III (Digital Instruments, constant force ≤10 nN). Each image required about 1.7 min (512 scans at 0.5 Hz). Therefore, since the effects of TBP were time-dependent, nuclei were fixed in 0.5% glutaraldehyde at the different test times (5–60 min). AFM imaging and patch clamp recordings were not carried out simultaneously.

## Results

### NPCs Interact With And Mediate TBP Translocation Into The Nucleus

Figure 1 illustrates the effects of 250 pM cytosolic TBP. In all the 6 patches tested at this concentration, TBP permanently opened the NPCs. The transcription factor also increased the number of open, ion-conducting channels (*see* Effects of TBP on Single NPC channel Stochastic Characteristics). In 9 of the 22 experiments carried out with 25–250 pM TBP, the NPC channels did not close at all, demonstrating a strong and permanent action of the nucleophilic protein on the channel gate(s). Lower TBP concentrations (2.5–125 fM) did not produce these effects. However, at lower concentrations, the long duration of the recordings demonstrated another function of the TATA-binding protein: that of conferring long-term stability to the NPC structure. As shown in Fig. 2A, at 125 fM TBP (n = 6), the recordings were stable for up to 58 hr, a length of time far beyond those reported for any patch clamp study but consistent with the observed long-lasting stabilizing effects of TBP on DNA (e.g., Conaway & Conaway, 1993). The lower concentrations of the transcription factor facilitated the detection of molecular translocation, as illustrated by the patch conductance, $\Gamma = i/V$, records of Fig. 2*B*, taken with 25 fM TBP (n = 6). Complete molecular translocation was detected at about 1 hr but, as shown in Fig. 2*B*, it could be accelerated by adding MgATP to the preparation. ATPγS, a nonhydrolyzable analogue of ATP, did not accelerate translocation (n = 3), indicating the participation of this

[1] As noted in the previous paper on TFs (Bustamante et al., 1995b), TBP is sold on the basis of its efficacy, expressed in terms of footprint units (fpu). Conversion of fpu to moles per liter was carried out by taking into account TBP molecular weight and the weight per vial provided by the manufacturer. Due to manufacturing and marketing practices, the values given here are likely to be underestimates.

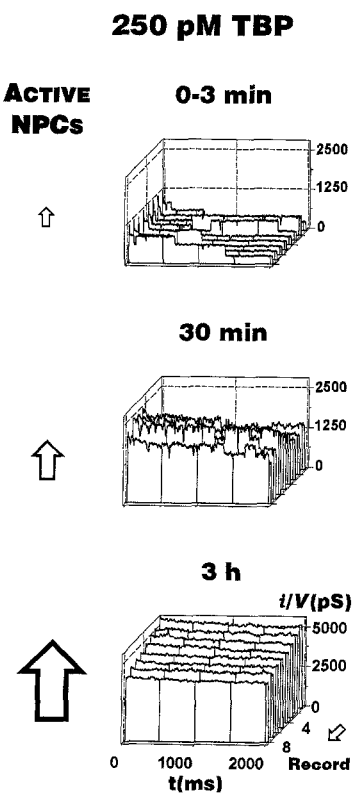


**Fig. 1.** TBP permanently opens NPC channels. Record ensembles of patch ion conductance, *i/V*, elicited with 2-sec pulses from 0 to −20 mV. The acquisition time for each record set is indicated on top of each plot. The patch clamp pipette contained 250 pM of TBP in control, high-K saline solution. Note the doubling in scale for the record ensemble at the bottom which was obtained at 3 hr. Assuming that the number of functional NPCs can be measured at the beginning of the pulse (t = 0 msec), one concludes that the number of active NPCs increased from 3 at 0–3 min, to 5 at 30 min, to 10 at 3 hr.

nucleotide hydrolysis. The double-stranded consensus oligonucleotide with TBP-binding sequence, used to determine whether the DNA-binding domain of the transcription factor was involved (*see* Materials and Methods), demonstrated no statistically significant difference in the response of NPC channel gating to TBP (n = 4, *not shown*).

### Effects of TBP on Single NPC Channel Stochastic Characteristics

The statistical behavior of NPC channel activity was analyzed as presented in the previous two companion papers (Bustamante et al., 1995*a,b*). Figure 3 illustrates our analysis for an experiment where the action of 250 pM TBP was tested. Relative values of the probability, $P_o$, of finding the population of $N$ channels open (each having an open probability of $p_o$; i.e., $P_o = Np_o$) were obtained from the current ensemble averages, $\langle i \rangle$. As discussed elsewhere (Bustamante, 1992; Bustamante et al., 1995*a,b*), under steady-state conditions the activity of NPC channels can be described with a binomial distribution (Bustamante, 1992). This observation supports the assumption that NPCs in a patch may be considered identical and functionally independent of each other (i.e., $P_o = Np_o$). More elaborate analysis of the TBP effects on channel statistical behavior is outside the aim of this paper (*see, for example,* Manivannan et al., 1992; Ramanan & Brink, 1993). The graph in Fig. 3*A* was generated from the 54 record ensembles of the experiment. The graph shows the progressive increase in patch average on conductance, $\langle i \rangle / V$, for the 4 voltage levels used in this experiment: ±10 and ±40 mV. Figure 3*B* shows the typical linear relationship between the discrete current jumps, $\Delta i$, and the applied voltage, $V$ (*see* Bustamante, 1992). Figure 3*C* depicts the time course of $P_o$ during the experiment. The values were obtained by dividing the average conductance in Fig. 3*A* by the single channel conductance measured for each ensemble. Figure 3*D* shows the same plot normalized in relation to the maximum at the end of the experiment.

Figure 4 highlights the results from another experiment in which 25 pM TBP was used. Figure 4*A* shows the time course of average patch conductance derived from the 34 current ensembles generated during this experiment. The initial reduction in patch conductance was followed by a permanent increase. Figure 4*B* illustrated the time course of TBP action on single NPC channel conductance, $\gamma$. The reduction in conductance was reversed by application of 2 mM ATP to the bath. This effect is similar to that shown by the records in Fig. 2. The effect was indirect and likely the result of the ATP molecules having free access to the nucleoplasm (i.e., to the nuclear pores) during the NPC channel openings. The quantized or discrete jumps between open and closed configurations of the channel were not observed in 14 ensembles during channel plugging and during permanent channel opening (shaded areas). This led to a reduced but sufficient number of data points describing the events (n = 20). Figure 4*C* shows the single channel current-voltage relationship in a fashion similar to that of Fig. 3*B*. Finally, the time course of relative $Np_o$ was calculated from the data in Fig. 4*A* with the conductance values shown in panel *B*.

We compiled the TBP-induced changes in single channel conductance, $\gamma$, from experiments where the open-close state transitions could be resolved. At <25 pM, the changes were not statistically significant, whereas at 125 pM the changes amounted to 1.25 ± 0.08 ($n$ = 11, mean ± SD, $P < 0.0001$). The bar graph in Fig. 5*A* shows the changes for 125 pM TBP. A graph illustrating the effects on $Np_o$ is given in Fig. 5*B*. The values were normalized in relation to the final value. At the start of the experiments, $Np_o$ was 0.24 ± 0.11. The value then decreased to 0.03 ± 0.11 during macromolecular plugging, and then increased to attain the maximum nor-

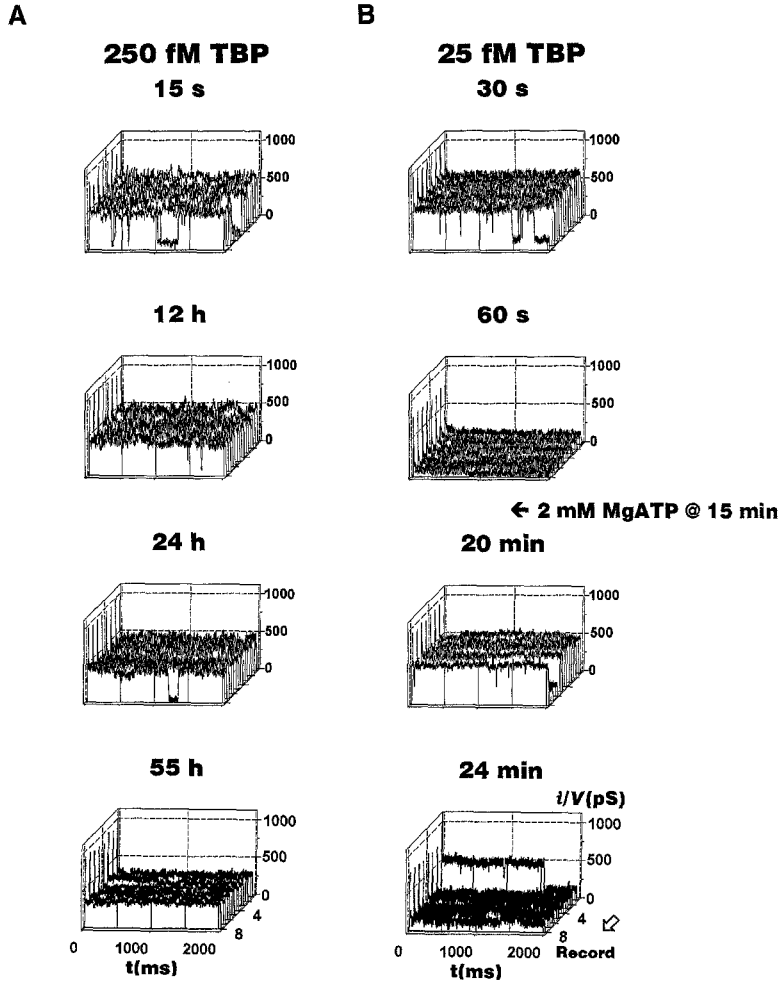


**Fig. 2.** TBP stabilizes NPCs and reduces NPC channel conductance during translocation. (*A*) NPC stabilization by 250 fM TBP. The unusual long-lasting life of the preparation demonstrates the stability conferred by TBP to NPCs. (*B*) NPC conductance, $\gamma$, is reduced during translocation of TBP molecules at 25 fM. TBP translocation was assisted by adding 2 mM ATP to the bath at 15 min. As the ATP molecule passed readily through the pores, it is assumed that ATP reached the NPC in less than 1 min. Note that the next translocation, at 24 min, caused the next reduction of $\gamma$.

malized value of 1. We indicated above that at concentrations greater than 250 pM, channel closures were not detected and that at lower concentrations the channel behavior showed a different mode of operation. Therefore, it is not possible for us to give other than a range of 25–250 pM for the binding constant ($K_d$) of a putative TBP-NPC site for chemical interaction. Low TBP concentrations caused an alternating behavior in the average ion conductance of the patch suggesting macromolecular translocations. Figure 6 demonstrates that despite the obvious stabilizing effect of 1 pM TBP on NPC channel gating, the patch conductance fluctuated between low and high periods which we associated with sporadic translocation of the highly dilute TBP solution (*see* Discussion).

## TBP Molecules Bind And Open NPCs

Figure 7 illustrates the results of AFM imaging. As shown in Fig. 7, AFM revealed that the TBP molecules attached to the cytoplasmic ring of the NPCs. Figure 7*A* shows an NPC in control conditions. The image has all the known topological features of the cytosolic side of NPCs (e.g., Panté & Aebi, 1994). Figure 7*B* shows an image of an NPC after 5 min exposure to 1 pM TBP. Here we see a TBP molecule sitting in the outer rim of the pore. The image in Fig. 7*B* agrees with our patch clamp observations on the timing of the onset of TBP effects (*see* Fig. 1) and also agrees with biochemical studies of the time taken for *O*-GlcNAc addition to NPCs (Davis & Blobel, 1987). However, when the images from all tests were pooled, we could not obtain a definitive answer as to the effects of TBP on channel diameter for two reasons. First, due to the principle of operation of the AFM (a scanning probe), in many images the accumulation of TBP molecules on the NPC rim interfered with the imaging of the channel interior, making the measurements of channel diameter unreliable. Second, the mean of channel diameter dilation (obtained from the channels that were reliably resolved) was not statistically significant (a reflection of the moderate change in single channel conductance, $\gamma$, *see* Fig. 5). Figure 7*C* shows an NPC after 1 hr exposure to the

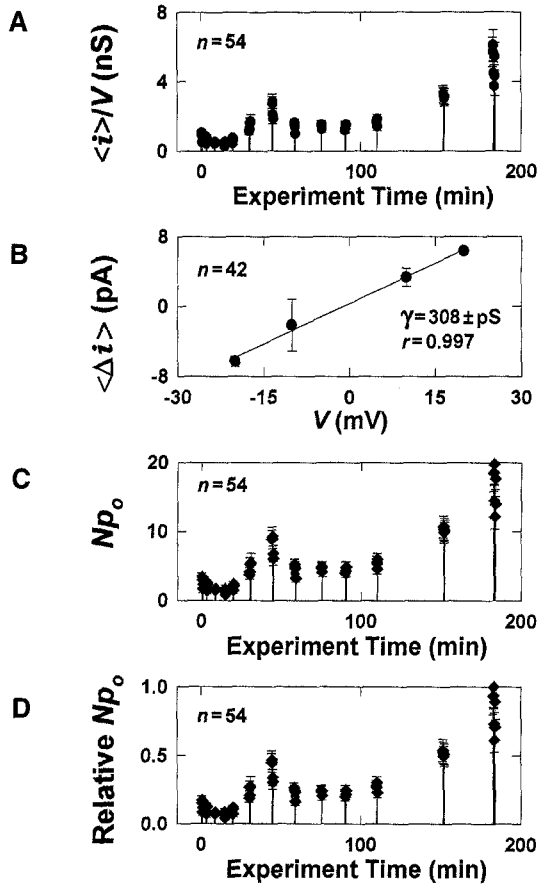


**Fig. 3.** Effects of 250 pM TBP on the stochastic behavior of nuclear pore ion channel activity. (*A*) Time course of patch average ion conductance. Current traces, $i(t)$, were averaged, $\langle i \rangle$, in each ensemble to obtain average conductance, $\langle i \rangle / V$. The drop-lines graph illustrates the time course of mean ion conductance following exposure to 250 pM TBP. A total of 54 ensembles were generated in this experiment. Superimposed to the data points are their corresponding standard deviations. (*B*) Single channel current-voltage relationship. Single channel conductance, $\gamma$, was obtained from the relationship between the current jumps, $\Delta i$ (from the nonconducting to the conducting states: closed and open), and the applied voltage, $V$. The data points represent the mean values, $\langle \Delta i \rangle$, for each voltage. A total of 42 points were obtained from well-defined (>100 msec) state transitions in the 54 current ensembles of this experiment. Standard deviations bars have been superimposed to the data points. (*C*) Time course of open probability $P_o$, or $Np_o$, for the channel population in the patch (with $N$ representing the number of channels in the patch and $p_o$ the open probability of a single channel). The probability was estimated by dividing the values in (*A*) by the single channel conductance, $\gamma$, evaluated for the corresponding ensemble average. (*D*) Graph constructed with the values in (*C*) normalized with respect to the final maximal value.

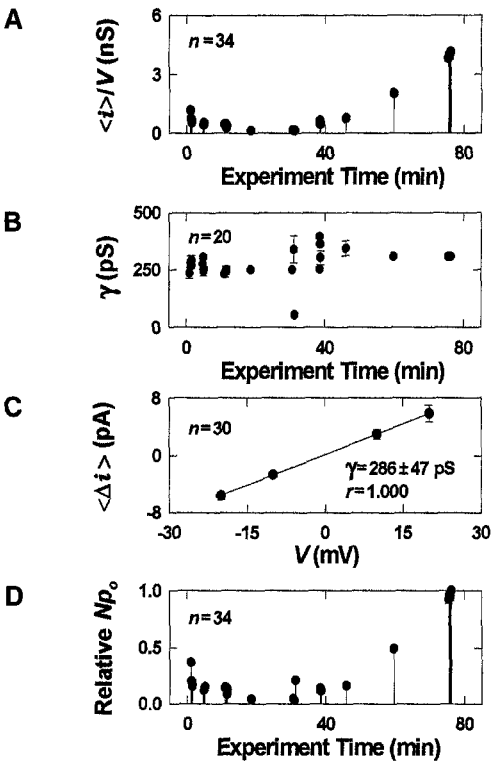


**Fig. 4.** Effect of 25 pM TBP on single NPC channel gating properties. (*A*) Time course of average patch ion conductance under the action of 25 pM TBP. A total of 34 ensembles were generated and analyzed during this experiment. Error bars giving the respective standard deviations, superimpose the data points. (*B*) Time course of average single channel conductance. Discrete jumps between open and closed configurations of the channel were not resolved in 14 ensembles during channel plugging and during permanent channel opening (shaded areas). Therefore, the number of data points describing the events was lower than the total number of ensembles (i.e., 20 rather than 34). (*C*) Plot of the means of single current jumps *vs.* applied voltage. (*D*) Time course of $Np_o$ calculated with the conductance values shown in *B*.

protein. It is evident that the cytosolic surface of the NPC doubled its size due to the increased number of TBP molecules attached to it (note the doubling of the scale). Panels *D* and *E* in this figure are control images of TBP molecules on poly-L-lysine. Poly-L-lysine was needed as a substrate to immobilize the TF molecules which would otherwise be dragged by the AFM tip during scanning. Figure 7*D* is an image of the substrate, demonstrating that it is a smooth layer and that it did not produce artifactual images. Figure 7*E* is an image of the TBP on the poly-L-lysine substrate showing TBP particles and demonstrating the capacity of TF molecules to aggregate. The bar graph in Fig. 8 shows the means and standard deviations of the diameter of NPC periphery measured from the AFM images at 0, 5 and 60 min under control (C) and test (TBP) conditions. The number of nuclei used in each group (# Nuclei) and the number of NPCs imaged per group (# NPCs) are shown on the top of the graph. Although the pooled data at 5 min were not statistically significant ($P = 0.25$), the effects were significant at 60 min ($P < 0.00001$). This indicates that from 5 to 60 min the diameter of the NPC periphery progressively increased.

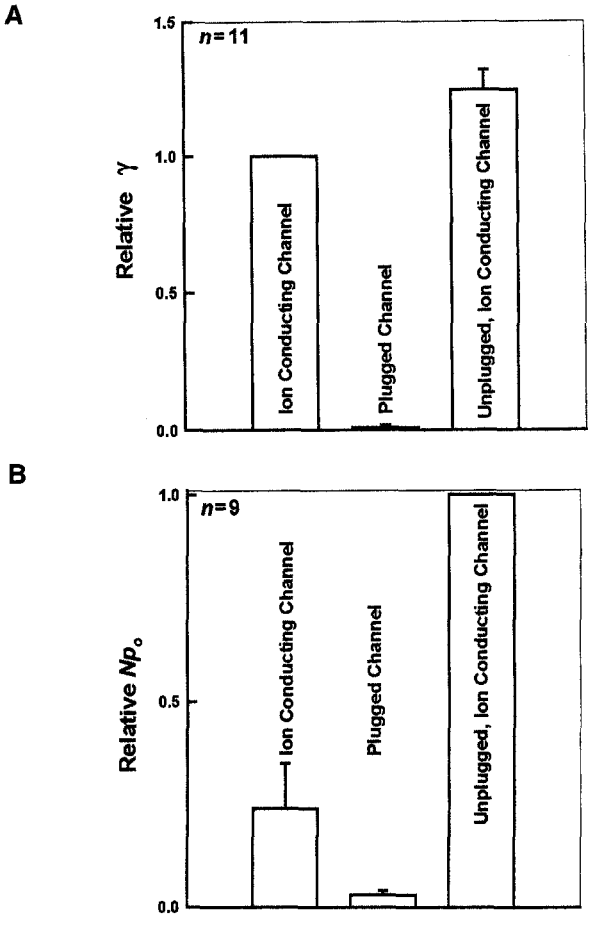


**Fig. 5.** TBP action on single NPC channel conductance, $\gamma$, and open probability of the patch channel population, $Np_o$. (*A*) Relative changes in $\gamma$ (mean ± SD) before, during, and after translocation of TBP molecules at 125 pM in 11 patches. (*B*) Relative $Np_o$ (mean ± SD) normalized to the final activity following TBP translocation. A total of 9 patches were analyzed.

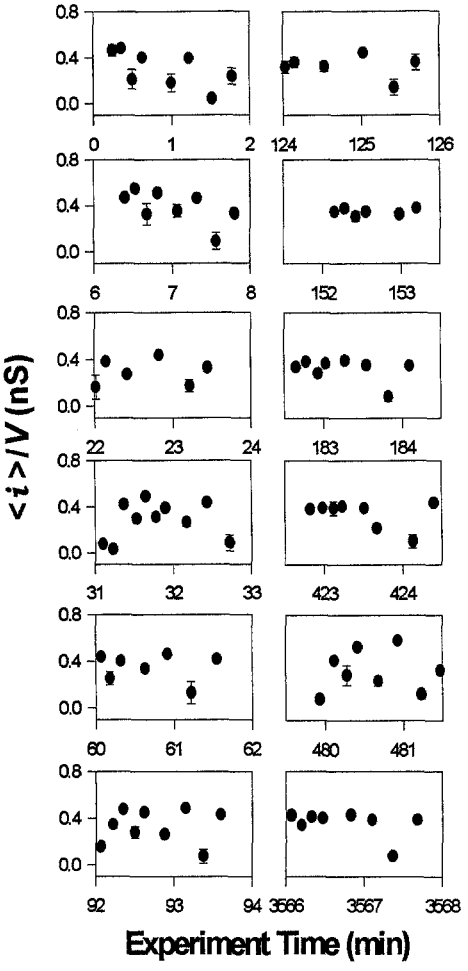


**Fig. 6.** Effect of 1 pM TBP on average patch ion conductance. Plots of patch average ion conductance at different times during a long-lasting experiment (>48 hr). The plots illustrate the alternating behavior of the patch conductance. The low conductance values are associated with plugging of the NPC channel during translocation. High values are attributed to unplugged NPC channel.

## Discussion

### NPCs Interact With And Mediate TBP Translocation Into The Nucleus

Prevalent schemes of gene regulation by transcription factors neglect the potential interactions of these nucleophilic proteins with NPCs. We have shown here, with patch clamp and AFM, that during their nucleocytoplasmic translocation, TBP molecules interact not only with the interior lining of NPC channels (mostly through pure mechanical forces) but that they also attach and/or bind to the cytoplasmic face of the NPCs (physically and/or chemically). *O*-GlcNAc glycosylation of transcription factors has been proposed as an important regulatory mechanism in transcription (e.g., Jackson & Tjian, 1988; Swillens & Pirson, 1994). *O*-GlcNAc glycosylation levels are known to increase in the nucleus during periods of cell stimulation (Hart et al., 1989; Haltiwanger et al., 1992*a,b*). Therefore, since major NPC proteins are *O*-GlcNAc glycosylated and have many available *O*-GlcNAc glycosylation sites, we propose that the *O*-GlcNAc moiety likely mediates TBP-NPC interactions. That is, through *O*-GlcNAc glycosylation, TBP prepares the NPC for demanding macromolecular translocations during cell phases of increased transcriptional activity. This type of architectural role of TFs is now recognized (e.g., Wolffe, 1994). The effective concentration range of TBP is similar to that reported in biochemical studies of this transcription factor (Imbalzano et al., 1994). The higher sensitivity of our detection system (both patch clamp and AFM), however, allowed us to dissect the fine details of TBP action on NPC gating properties and structure (*see* Simon & Blobel, 1991, 1992; Bezkurov et al., 1994; Bustamante et al., 1995*b*).

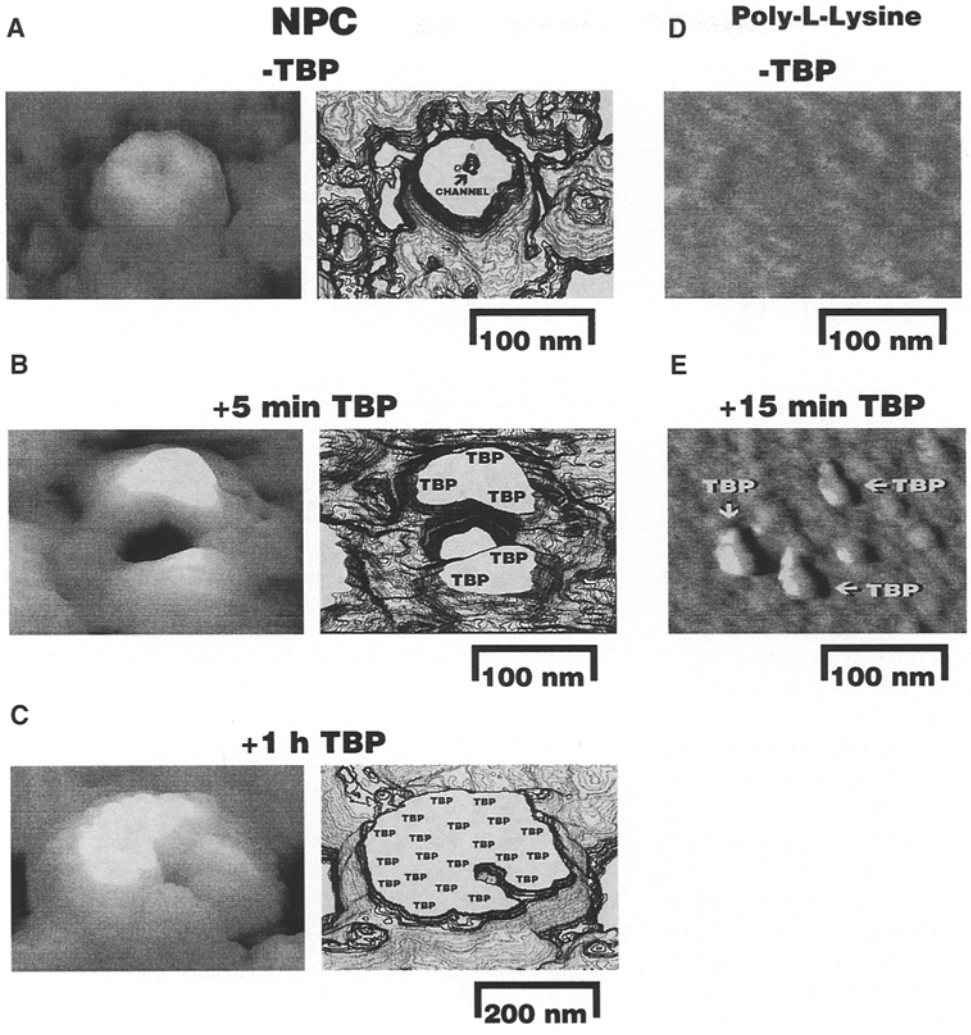


**Fig. 7.** TBP molecules bind to the cytoplasmic face of NPCs as demonstrated by atomic force microscopy, AFM. (*A–C*) NPC images (left panels) and their respective contour maps (right panels). (*A*) NPC prior to TBP exposure. The NPC translocating channel is indicated with the arrow in the contour map. (*B–C*) NPC after 5 min and 1 hr exposure to 1 pM TBP. Note the doubling of the scale in *C*. Aggregates/multimers of TBP molecules are indicated with the label TBP. (*D,E*) Images of TBP molecules on poly-L-lysine were acquired to aid in their identification from images containing NPCs (e.g., *B,C*). The TBP molecules multimerized into macromolecular complexes that correspond to the features seen in *B* and *C*. Three of these complexes are indicated with arrows.

Our measurements of single channel conductance, $\gamma$, and our analysis of the single channel statistical properties (e.g., $P_o = Np_o$) suggest that the increased patch average ion conductance (*see* Figs. 3*A* and 4*A*) is due, in major part, to an upregulation in $Np_o$ (e.g., Fig. 3*C*) and, to a lesser extent, to a small increase in $\gamma$. Since our patches had an initial low count of operating channels, the TBP-induced increase in $P_o$ suggests that TBP activated channels which were initially in a dormant/inactive state (caused by an unknown mechanism such as phosphorylation/dephosphorylation) or initially plugged by macromolecules. As discussed in the previous paper (Bustamante et al., 1995*b*), despite the low concentration levels used, TBP molecules were in contact with the cytoplasmic side of the NPCs within the first seconds of recording. Therefore, the substantial increase in $P_o$ can be interpreted not as the recruitment or synthesis of NPCs (because substrates were absent) but as the unplugging and, thus the availability, of NPC channels for ion flow following complete macromolecular translocation.

TBP consists of several domains (e.g., Peterson et al., 1990; Struhl, 1994; Tjian & Maniatis, 1994). As a karyophilic protein, TBP contains at least one amino acid sequence acting as a nuclear localization signal (NLS, *see* Boulikas, 1994). We have shown (Bustamante et al., 1995*a*) that synthetic analogs of the SV40 large T antigen NLS do not affect NPC channel gating. Therefore, although we did not test the nuclear localization signal of

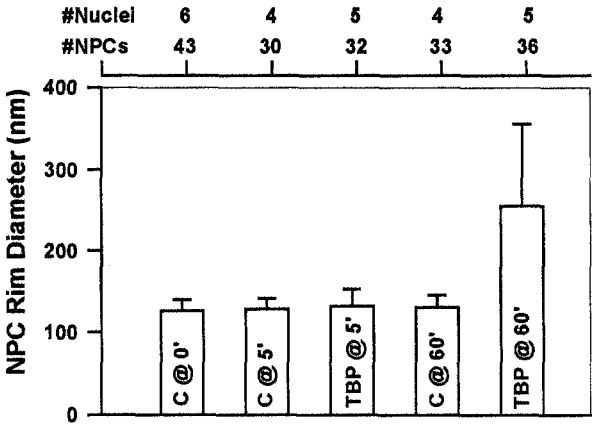


**Fig. 8.** Statistics of TBP effects on diameter of NPC Perimeter images with AFM. Bar graph showing the means and standard deviations of NPC diameters measured from AFM images under control (*C*) and test conditions (TBP, 1 pM) at 0, 5 and 60 min. The number of nuclei (# Nuclei) used for each group of measurements as well as the number of NPCs imaged per group (# NPCs) is given on the top axis of the graph.

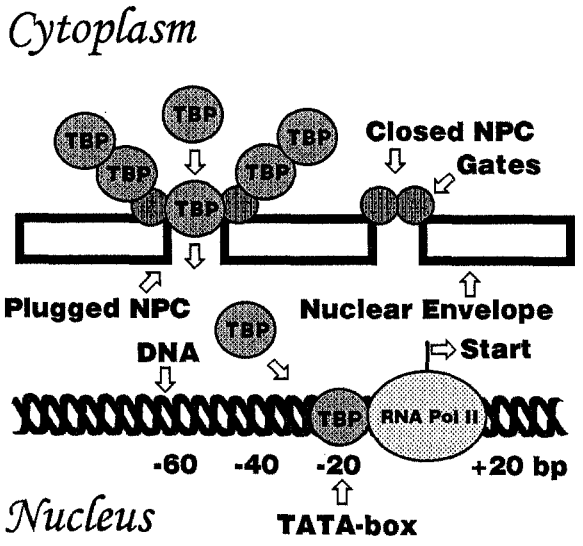


**Fig. 9.** Proposed paradigm to explain TBP-NPC interactions. When unplugged by translocating macromolecules, the NPC channels open and close according to the functional status of the cell, thus regulating the flow of monoatomic, monovalent ions like $K^+$. Upon arrival to the cytoplasmic side of the NPC, the TBP molecules interact with the channel, stabilizing them and favoring their opening. When present at relatively high concentrations (e.g., under conditions that stimulate TBP synthesis), the transcription factor molecules chemically bind to the NPC. At low, homeopathic concentrations, Newtonian mechanics and Brownian statistics principles govern the translocation of single molecules. During translocation of TBP molecules along the NPC channels, the molecules plug the channels for a length of time that depends on transport substrates, cytosolic signals and mechanical interactions between the molecules and the inner lining of the NPC channels (e.g., friction). Upon conclusion of translocation to the nuclear interior, the TBP molecules bind to their specific TATA-box located 20 base pairs upstream of the transcription startpoint (at which RNA polymerase II binds, assigned a +1 value). Numbers along the double-stranded DNA indicate base pairs from the transcription start site.

TBP, there is sufficient experimental evidence in our preparation suggesting that the TBP localization signal was not directly involved in the observed phenomena. The lack of action of the double-stranded consensus oligonucleotide with TBP-binding sequence indicates that the DNA-binding domain of TBP played no significant role in TBP-NPC interactions. As the consensus oligonucleotide was 25 base-pairs long, the calculated size of the TBP-oligonucleotide complex was 54.2 kD. These observations give further support to our interpretation that TBP-NPC interaction takes place at the cytoplasmic side of the nuclear pores and that a TBP domain distinct from those committed to nuclear localization and DNA-binding participated in this interaction.

### Translocating TBP Molecules Play The Role Of NPC Plugs

NPC channel activity at low TBP concentration is relevant because it follows the behavior expected for macromolecular translocation (e.g., Bezkurov et al., 1994; Bustamante et al., 1995*a,b*). High and low values of average patch ion conductance (*see* Fig. 6) correspond, respectively, to periods during which either ions or molecules were transported along the NPC channel (with the macromolecules acting as temporary channel plugs). Although the concentration level at which TBP conferred NPC stability is similar to that reported to biochemical studies (e.g., Conaway & Conaway, 1993), the low occurrence of low of patch ion conductance may be related to the high dilution used (*see* Bustamante et al., 1995*b*). Since the increase in $Np_o$ observed at the higher concentration range (25–250 pM) was not seen with the lower concentrations (2.5–125 fM), it is possible that access to the binding site was made more difficult due to the molecular displacements governed by the principles of Brownian motion (i.e., random walk mostly influenced by thermal energy). In other words, the effects of TBP observed at higher concentrations were dominated by chemical principles whereas those recorded at lower, homeopathic concentrations followed the principles of Newtonian mechanics and Brownian statistics.

Our AFM images did not display the prominent NPC plug (*reviewed in* Panté & Aebi, 1994) and this agrees with our patch clamp observations indicating that the plug is not a fixture of the NPC but a translocating macromolecule (*see* Figs. 2–4; *see also* Bustamante et al., 1995*a*). Since the scanning probe of the AFM could not enter the NPC channel, arguments about the existence of an NPC plug, based solely on AFM images are speculative. On the basis of the patch clamp results presented in this and the companion papers (Bustamante et al., 1995*a,b*) as well as of EM observations from other

laboratories (e.g., Panté & Aebi, 1994), we think that the presence of ATP during the AFM tests facilitated TBP translocation, thus reducing the chance of finding an AFM image with a TBP molecule in the cytoplasmic mouth of the NPC channel. Our interpretation agrees with electron microscopy (EM) observations showing that the plug is absent when EM specimens are prepared in the presence of ATP (e.g., Panté & Aebi, 1994). The accumulation of TBP molecules at the cytosolic side of the NPC is consistent with the multimerizing capacity of TBP (Kato et al., 1994; Tjian & Maniatis, 1994) and other *O*-GlcNAc glycoproteins (Hart et al., 1989; Haltiwanger et al., 1992*a,b*).

The results presented in this paper, and summarized in Fig. 9, are the first direct demonstration that NPCs mediate TBP regulation of gene activity and expression and that TBP directly interacts with NPCs and modifies their structure and function. These observations have potential applications in the design of new drugs aimed at manipulating the processes that participate in gene function. Such processes include signal transduction to the nucleus, transcriptional control and mRNA export, all of which are significant to the genesis of cell pathologies.

Supported by grants from the American Heart Association, Maryland Affiliate, to JOB, from the Medical Research Council of Canada to AL, from Research to Prevent Blindness to RAP, from National Institutes of Health Intramural Funding to JAH, and from the Deutsche Forschungsgemeinschaft, SFB 176 (A 6) to HO. The authors thank Peggy Kopps of Promega for her assistance in the calculation of TBP concentration and in finding biochemical applications where the transcription factor displays equally strong stabilizing effects.

## References

Bezkurov, S.M., Vodyanoy, I., Parsegian, V.A. 1994. Counting polymers moving through a single ion channel. *Nature* **370:**279–281

Binning, G., Quate, C.F., Gerber, Ch. 1986. Atomic force microscope. *Phys. Rev. Lett.* **56:**930–933

Boulikas, T. 1994. Putative nuclear localization signals (NLS) in protein transcription factors. *J. Cell. Biochem.* **55:**32–58

Braunstein, D., Spudich, A. 1994. Structure and activation dynamics of RBL-2H3 cells observed with scanning force microscopy. *Biophys. J.* **66:**1717–172

Buratowski, S. 1994. The basics of basal transcription of RNA polymerase II. *Cell* **77:**1–3

Bustamante, J.O. 1992. Nuclear ion channels in cardiac myocytes. *Pfluegers Arch.* **421:**473–485

Bustamante, J.O. 1993. Restricted ion flow at the nuclear envelope of cardiac myocytes. *Biophys. J.* **64:**1735–1749

Bustamante, J.O. 1994*a*. Open states of nuclear envelope ion channels in cardiac myocytes. *J. Membrane Biol.* **138:**77–89

Bustamante, J.O. 1994*b*. Nuclear electrophysiology. *J. Membrane Biol.* **138:**105–112

Bustamante, J.O., Hanover, J.A., Liepins, A. 1995*a*. The ion channel behavior of the nuclear pore complex. *J. Membrane Biol.* **146:**

Bustamante, J.O., Liepins, A., Hanover, J.A. 1994. Nuclear pore complex ion channels. *Mol. Membr. Biol.* **11:**141–150

Bustamante, J.O., Oberleithner, H., Hanover, J.A., Liepins, A. 1995*b*. Patch-clamp detection of transcription factor translocation along the nuclear pore complex channel. *J. Membrane Biol.* **146:**

Conaway, R.C., Conaway, J.W. 1993. General initiation factors for RNA polymerase II. *Annu. Rev. Biochem.* **62:**161–190

Davis, L.I., Blobel, G. 1987. Nuclear pore complex contains a family of glycoproteins that includes p62: glycosylation through a previously unidentified cellular pathway. *Proc. Natl. Acad. Sci. USA* **84:**7552–7556

Engel, A. 1991. Biological applications of scanning probe microscopes. *Annu. Rev. Biophys. Chem.* **20:**79–108

Greenblatt, J. 1992. Riding high on the TATA box. *Nature* **360:**16–17

Haltiwanger, R.S., Blomberg, M., Hart, G.W. 1992. Glycosylation of nuclear and cytoplasmic proteins. *J. Biol. Chem.* **267:**9005–9013

Haltiwanger, R.S., Kelly, W.G., Roquemore, E.P., Blomberg, M., Dong, L.-Y.D., Kreppel, L., Chou, T.-Y., Hart, G.W. 1992. Glycosylation of nuclear and cytoplasmic proteins is ubiquitous and dynamic. *Biochem. Soc. Trans.* **20:**264–269

Hart, G.W., Haltiwanger, R.S., Holt, G.D., Kelly, W.G. 1989. Glycosylation in the nucleus and cytoplasm. *Annu. Rev. Biochem.* **58:**841–874

Hernandez, N. 1993. TBP, a universal eukaryotic transcription factor? *Genes Dev.* **7:**1291–1308

Hoffman, M. 1993. The cell's nucleus shapes up. *Science* **259:**1257–1259

Hoh, J.H., Hansma, P.K. 1992. Atomic force microscopy for high-resolution imaging in cell biology. *Trends Cell Biol.* **2:**208–213

Hoh, J.H., Lal, R., John, S.A., Revel, J.-P., Arnsdorf, M.F. 1991. Atomic force microscopy and dissection of gap junctions. *Science* **253:**1405–1408

Hoh, J.H., Sosinsky, G.E., Revel, J.-P., Hansma, P.K. 1993. Structure of the extracellular surface of the gap junction by atomic force microscopy. *Biophys. J.* **65:**149–163

Holt, G.D., Snow, C.M., Senior, A., Haltiwanger, R.S., Gerace, L., Hart, G.W. 1987. Nuclear pore complex glycoproteins contain cytoplasmically disposed O-linked *N*-acetylglucosamine. *J. Cell. Biol.* **104:**1157–1164

Hori, R., Carey, M. 1994. The role of activators in assembly of RNA polymerase II transcription complexes. *Curr. Opin. Gen. Dev.* **4:**236–244

Horikoshi, M., Wang, C.K. Fujii, H., Cromlish, J.A., Weil, P.A., Roeder, R.G. 1989. Cloning and structure of a yeast gene encoding a general transcription initiation factor TFIID that binds to the TATA box. *Nature* **341:**299–303

Imbalzano, A.N., Zaret, K.S., Kingston, R.E. 1994. Transcription factor (TF) IIB and TFIIA can independently increase the affinity of the TATA-binding protein for DNA. *J. Biol. Chem.* **269:**8280–8286

Jackson, S.P., Tjian, R. 1988. O-glycosylation of eukaryotic transcription factors: implications for mechanisms of transcriptional regulation. *Cell* **55:**125–133

Kato, K., Makino, Y., Kishimoto, T., Yamauchi, J., Kato, S., Muramatsu, M., Tamura, T. 1994. Multimerization of the mouse TATA-binding protein (TBP) driven by its C-terminal conserved domain. *Nucleic Acids Res.* **22:**1179–1185

Kim, J.L., Burley, S.K. 1994. 1.8 A resolution refined structure of TBP recognizing the minor groove of TATAAAAG. *Struct. Biol.* **1:**638–653

Klein, C., Struhl, K., 1994. Increased recruitment of TATA-binding protein to the promoter by transcriptional activation domains in vivo. *Science* **266:**280–282

Kokubo, T., Gong, D.W., Wooton, J.C., Hoikoshi, M., Roeder, R.G., Nakatani, Y. 1994. Molecular cloning of Drosophila TFIID subunits. *Nature* **364:**484–487

Lal, R., John, S.A. 1994. Biological applications of atomic force microscopy. *Am. J. Physiol.* **266:**C1–C21

Lal, R., Kim, H., Garavito, R.M., Arnsdorf, M.F. 1993. Imaging of reconstituted biological channels at molecular resolution by atomic force microscopy. *Am. J. Physiol.* **265:**C851–C856

Lal, R., Yu, L. 1993. Atomic force microscopy of cloned nicotinic acetylcholine receptor expressed in *Xenopus oocytes. Proc. Natl. Acad. Sci. USA* **90:**7280–7284

Lewin, B. 1990. Commitment and activation at pol II promoters. *Cell* **61:**1161–1164

Lian, J.B., Stein, G.S., Bortell, R., Owen, T.A. 1991. Phenotype suppression: a postulated molecular mechanism for mediating the relationship of proliferation and differentiation by Fos/Jun interactions at AP-1 sites in steroid responsive promoter elements of tissue-specific genes. *J. Cell Biochem.* **45:**9–14

Manivannan, K., Ramanan, S.V., Mathias, R.T., Brink, P.R. 1992. Multichannel recordings from membranes which contain gap junctions. *Biophys J.* **61:**216–227

Marx, J. 1993. Forging a path to the nucleus. *Science* **260:**1588–1560

Miller, M., Park, M.K., Hanover, J.A. 1991. Nuclear pore complex: structure, function and regulation. *Physiol. Rev.* **71:**681–686

Morris, V.J. 1994. Biological applications of scanning probe microscopies. *Prog. Biophys. Mol. Biol.* **61:**131–185

Nebert, D.W. 1994. Drug-metabolizing enzymes in ligand modulated transcription. *Biochem. Pharmacol.* **47:**25–37

Nikolov, D.B., Burley, S.K. 1994. 2.1 A resolution refined structure of a TATA box-binding protein (TBP). *Struct. Biol.* **1:**621–637

Oberleithner, H., Birnckmann, H., Schwab, A., Khrone, G. 1994. Imaging nuclear pores of aldosterone sensitive kidney cells by atomic force microscopy. *Proc. Natl. Acad. Sci. USA* **91:**9784–9788

Oberleithner, H., Giebisch, G., Geibel, J. 1993. Imaging the lamellipodium of migrating epithelial cells *in vivo* by atomic force microscopy. *Pfluegers Arch.* **425:**401–407

Panté, N., Aebi, U. 1994. Towards understanding the three-dimensional structure of the nuclear pore complex at the molecular level. *Curr. Opin. Struct. Biol* **4:**187–196

Parker, T.G., Schneider, M.D. 1991. Growth factors, proto-oncogenes, and plasticity of the cardiac phenotype. *Annu. Rev. Physiol.* **53:**179–200

Peterson, M.G., Tanese, N., Pugh, B.F., Tjian, R. 1990. Functional domains and upstream activation properties of cloned human TATA binding protein. *Science* **248:**1625–1630

Peterson, M.G., Tupy, J.L. 1994. Transcription factors: a new frontier in pharmaceutical development. *Biochem. Pharmacol.* **47:**127–128

Prabhakar, P., Kayastha, A.M. 1994. Mechanism of DNA-drug interactions. *Appl. Biochem. Biotech.* **47:**3955

Radmacher, M., Tillmann, R.W., Firtz, N., Gaub, H.E. 1992. From molecules to cells-imaging soft samples with the AFM. *Science* **257:**1900–1905

Ramanan, S.V., Brink, P.R. Multichannel recordings from membranes which contain gap junctions. II. Substates and conductance shifts. *Biophys. J.* **65:**1387–1395

Rutgar, D., Hansma, P.K. 1990. Atomic force microscopy. *Phys. Today* **43:**23–30

Rowlands, T., Baumann, P., Jackson, S.P. 1994. The TATA-binding protein: a general transcription factor in eukaryotes and archaebacteria. *Science* **264:**1326–1329

Sadoshima, J.-I., Jahn, L., Takahashi, T., Kulik, T.J., Izumo, S. 1992. Molecular characterization of the stretch-induced adaptation of cultured cardiac cells: an *in vitro* model of load-induced cardiac hypertrophy. *J. Biol. Chem.* **267:**10551–10560

Simon, S.M., Blobel, G. 1991. A protein-conducting channel in the endoplasmic reticulum. *Cell* **65:**371–380

Simon, S.M., Blobel, G. 1992. Signal peptides open protein-conducting channels in *E. coli. Cell* **69:**677–684

Struhl, K. 1994. Duality of TBP, the universal transcription factor. *Science* **263:**1103–1104

Sweillens, S., Pirson, I. 1994. Highly sensitive control of transcriptional actiaction by factor heterodimerization. *Biochem. J.* **301:**9–12

Tanese, N., Tjian, R. 1993. Coactivators and TAFs: a new class of eukaryotic transcription factors that connect activators to the basal machinery. *Cold Spring Harbor Symp. Quant. Biol.* **43:**179–185

Tjian, R., Maniatis, T. 1994. Transcriptional activation: a complex puzzle with few easy pieces. *Cell* **77:**5–8

Weis, L., Reinberg, D. 1992. Transcription by RNA polymerase II: initiator-directed formation of transcription-competent complexes. *FASEB J* **6:**3300–3309

Wolffe, A.P. 1994. Architectural transcription factors. *Science* **264:**1100–1101